Title

Rapid Assembly of Multifunctional Thin Film Sensors for Wind Turbine Blade Monitoring

Authors

Mortensen, Lars P

Ryu, Dong Hyeon

Zhao, Ying Jun

et al.

Publication Date

2013-10-04

DOI

10.4028/www.scientific.net/kem.569-570.515

Peer reviewed

Rapid Assembly of Multifunctional Thin Film Sensors for Wind Turbine Blade Monitoring

Lars P Mortensen[1], Donghyeon Ryu[2], Yingjun Zhao[2], and Kenneth J Loh[2,a]

[1]Department of Mechanical and Aeronautical Engineering, University of California, Davis, CA 95616, USA

[2]Department of Civil and Environmental Engineering, University of California, Davis, CA 95616, USA

[a]kjloh@ucdavis.edu

Keywords: carbon nanotubes, nanocomposite, spray fabrication, strain sensing, wind turbine.

Abstract. Wind is a competitive, clean, and fast-growing renewable energy industry. However, in order for wind to compete with fossil fuel-based energies, it is necessary to achieve lower cost of energy. One way is to reduce operations and maintenance costs by integrating structural health monitoring (SHM) systems with wind turbines. It has been found that the fiber-reinforced polymer (FRP) composite-based wind blades are susceptible to damage (*e.g.*, cracks, debonding, and impact). Damage is typically invisible to the naked eye and can propagate rapidly to cause sudden failure. This work presents a new SHM approach using embedded thin film sensors for detecting damage in FRP-based wind blades. While previous studies have shown that carbon nanotube-based thin films can be incorporated with FRPs for sensing, this study further investigates their electromechanical properties. First, a unique spray fabrication approach was employed so that films can be assembled on a low cost basis and can be deposited onto any substrate or structure. Second, the electrical properties of films subjected to post-fabrication thermal annealing were compared. Finally, freestanding films were prepared and subjected to uniaxial tensile cyclic loading while their resistivity was measured simultaneously. The results showed that these films were piezoresistive.

Introduction

Wind energy is one of the most popular renewable energy resources, particularly in Europe. In the U.S., California aims to have 33% of its electricity supply coming from renewable sources by 2020 [1], and the national target is 20% by 2030 solely from wind [2]. Despite its popularity and widespread adoption, wind energy has difficulty competing with conventional fossil fuel-based resources (*e.g.*, coal, natural gas, and nuclear) due to its high cost-of-energy (COE). In fact, up to 60% of its COE is attributed to operation and maintenance [3]. Extensive maintenance and monitoring of these structures are required due to their continuous operations and harsh operating environment. In many cases, routine inspections, repairs, or part replacements require the turbine to come offline, and extensive labor, equipment, and time are needed; all of these increase wind COE.

Among various components of a turbine, the wind blade (which is typically fabricated using glass fiber-reinforced polymer (GFRP) composites) is susceptible to damage. While GFRP offers a superior strength-to-weight ratio as compared to conventional metallic structural elements, GFRPs can sustain damage such as matrix cracking, debonding, and delamination [4]. In addition, damage is also prone to occur near the root of the blade (where it connects to the rotor) due to the high stresses. The concern of damage occurrence and potential catastrophic blade failure is becoming a greater concern as larger and longer blades are being designed, built, and placed in service [5]. Therefore, there is a dire need to monitor blade performance so that problems can be identified promptly and the necessary repairs performed. The end result can eventually lead to a decrease in wind COE.

Various structural health monitoring (SHM) techniques have been developed for monitoring composite wind blades, and many of them have been successfully adopted for other types of

structures [6]. Operational modal analysis is one of the most commonly used techniques to identify structural property changes (*e.g.*, due to damage). Structural dynamic response based on data from instrumented accelerometers can be used to determine stiffness degradation and/or boundary condition changes [7]. Instead of only measuring structural response to ambient excitations, piezoelectric transducers can act as both sensors and actuators to interrogate a structure on demand. Localized damage severity and its location can be identified using, for example, the impedance method [6, 7]. There are also non-contact sensors such as a laser Doppler vibrometer [7]. However, most of these methods are faced with challenges when applied to monitoring wind turbine blades. For example, accelerometers add significant weight, embedded piezoelectric transducers may serve as damage initiation sites, and other techniques may require the blade to remain stationary. Another limitation is that these sensors only measure data at their instrumented locations. Characterization of the entire blade's response to loads or for damage estimation relies upon interpolation between instrumented sensor locations.

A previous study by Loyola *et al.* [4, 8] has shown that piezoresistive carbon nanotube (CNT)-based thin films can be deposited on or embedded in GFRPs for *in situ* strain monitoring. When coupled with an electrical impedance tomography (EIT) algorithm, these "sensing skins" are able to measure the spatial distribution of strain [9]. Unlike conventional sensors, this technology permits the direct measurement of strain distribution, which can be employed for identifying the magnitude and location of damage due to deformation, cracks, and impact, among others. These CNT-based thin films have been fabricated using a layer-by-layer (LbL) method [8, 10]. While these nanocomposites possess a uniform and percolated morphology, strain sensitivity, and outstanding mechanical performance, the fabrication technique is time consuming and not scalable (*i.e.*, their assembly onto large structures remains challenging). Thus, an alternative fabrication method is needed so that these sensors can be transitioned from the lab to field implementations, particularly for embedment in full-scale wind blades for distributed strain monitoring and damage detection.

Thus, the objective of this study is to demonstrate a rapid CNT-based thin film fabrication method and to characterize its electromechanical response to applied strains. First, the details of using a spray fabrication method for depositing the nanocomposites will be discussed. Films have been sprayed onto glass microscope slides, and a subset of these films has been subjected to post-fabrication thermal annealing. Second, the electrical resistivity of annealed and non-annealed specimens has been compared. Their change in resistivity over time has also been studied. Then, scanning electron microscopy (SEM) has been used for assessing nanocomposite morphology and the dispersion of nanotubes deposited. This study concludes with characterizing the films' electro-mechanical response to applied tensile cyclic strains.

Spray Fabrication of Nanocomposites

The rapid assembly of CNT-based thin film sensors was achieved through the design of a spray fabrication process [11]. Unlike other fabrication methods such as LbL that require a long time to deposit micron-thick films (*i.e.*, on the order of days), this technique could fabricate homogeneous films in a manner of minutes. Other advantages are that it is scalable and versatile; in essence, they can be applied to virtually any structural surface of any size.

The fabrication process began with preparing an aqueous suspension of CNTs in a polyelectrolyte (PE) solution. Dispersion of nanotubes was required in order to take advantage of the unique electromechanical properties of CNTs [10]. First, a 2 *wt.*% poly(sodium 4-styrenesulfonate) (PSS) (*Mw* ≈ 1M*,* Sigma-Aldrich*)* solution was prepared in deionized (DI) water. Second, multi-walled carbon nanotubes (MWNT) were added to the PSS solution. High-molecular weight PSS was chosen as the PE for suspending CNTs, because Moore *et al.* [12] showed that it tends to suspend more CNTs due to its longer polymeric chains and the size of its hydrophilic groups. In addition, a small amount of N-methyl-2-pyrrolidinone (NMP) was also added to the mixture in order to facilitate dispersion [13]. Finally, the MWNT/PSS-NMP mixture was subjected to 60 min of high-energy tip sonication (6.35 mm tip, 225 W, 20 kHz).

Once the MWNTs were dispersed in the PSS-NMP solution, the next step was to prepare a poly(vinylidene fluoride) (PVDF)-based solution that could be used as is for spray fabrication. PVDF was added to the solution to help promote adhesion of the solution/film to the substrate. The low surface energy of PVDF enabled the solution to flow over and cover the substrate surface, thereby maximizing its contact area and surface adhesion [14]. Here, a Kynar PVDF with 150 nm-diameter spherical particles suspended in an Aquatec surfactant solution was added to the MWNT-based solution and was then diluted with DI water. The solution was stirred vigorously to mix its contents. The PVDF particles create a segregated network of CNTs [11]. The final solution, prior to spray deposition, consisted of 5 *wt*.% MWNTs. Due to the fact that nanotubes could agglomerate, these solutions were prepared immediately prior to spray fabrication.

Finally, the MWNT-based solution was employed for spraying approximately 20 to 30 films onto 75×25 mm^2 glass microscope slides. The solution was sprayed using an airbrush and was performed in a fume hood. After spraying, the specimens were left to air dry for 1 h. Fig. 1 shows a picture of a completed thin film. Although these films could be used as is, a portion of the films were annealed at temperatures ranging from 100 to 250 °C. Post-fabrication annealing was performed to remove any pre-existing defects and to increase their electrical conductivity [15]. The last step was to obtain a freestanding nanocomposite, which was achieved by immersing all films (annealed and non-annealed specimens) in DI water for ~1 min. Not only did water treatment remove the film from its substrate (which is potentially due to the fact that PSS is water soluble), but it also increased their electrical conductivity (again, due to removal of PSS).

Nanocomposite Morphology

The morphology of MWNT-based films deposited onto glass microscope slides was observed using an FEI 430 NanoSEM scanning electron microscope. The SEM specimens were affixed onto an SEM mount using carbon sticky dots. Fig. 2 shows two representative SEM images of the non-annealed nanocomposites. Fig. 2a shows the nanocomposite's surface, and one can observe that individual MWNTs were uniformly dispersed and embedded within the PSS/PVDF matrix. Also, the MWNTs exceeded its percolation threshold, thereby forming electrically conductive pathways. A representative cross-sectional image is shown in Fig. 2b. In Fig. 2b, it can be observed that the MWNT-based film layer was uniformly coated over the glass substrate. Fig. 2b also supports that the spray fabrication technique can yield films with uniform thicknesses. Using similar measurements shown in Fig. 2b, it was determined that the average thickness was 10 μm. This measure of average thickness was used for calculating electrical resistivity, as will be shown in the following sections.

Nanocomposite Electrical Properties

One of the main goals of this study was to investigate the electrical properties of this sprayed MWNT-based thin film. First, the effect of post-fabrication thermal annealing (and the annealing temperature used) was investigated to see how it affects bulk film resistivity. Second, the stability

Figure 1: The MWNT-based film was sprayed onto a 75×25 mm^2 glass microscope slide before conducting water treatment.

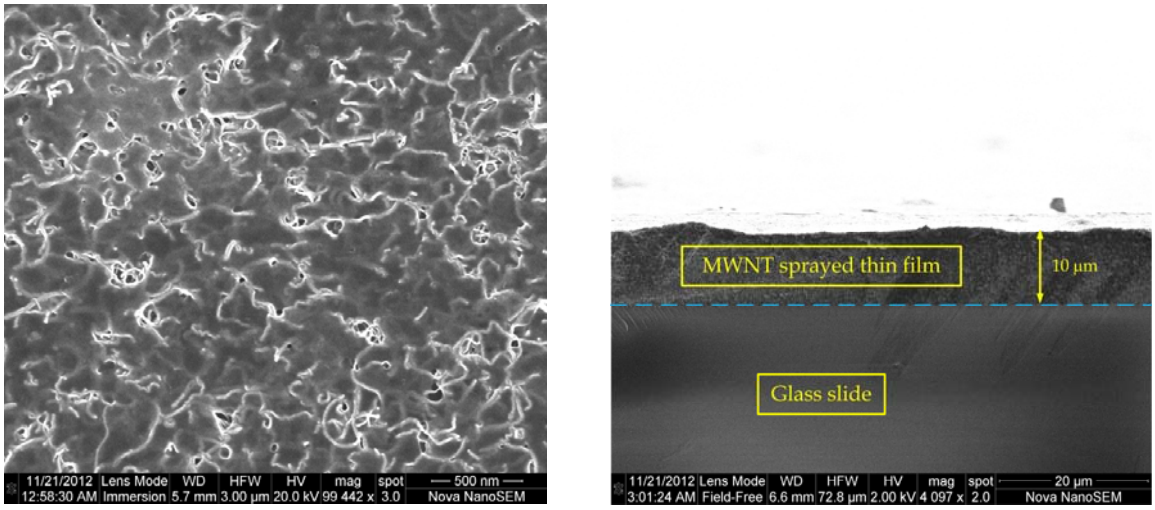

(a) (b)

Figure 2: (a) The SEM image of the nanocomposite surface shows that MWNTs are adequately dispersed within the PSS/PVDF matrix and has exceeded its percolation threshold. (b) The cross-sectional SEM image shows that the spray fabrication method can yield films with uniform thickness of approximately 10 μm.

of their electrical properties with respect to time has also been investigated by measuring resistivity over a period of several hours. Experimental methods and the results will be discussed as follows.

Effects of Thermal Annealing. Film specimens were prepared using the spray fabrication method and annealed at temperatures ranging from 100 to 250 °C, as described earlier. A subset of films was not annealed to form the control set. It should be mentioned that, even though films deposited onto the glass substrates were used, all films were treated with water prior to testing. This ensured that films were subjected to the same fabrication steps as those freestanding films used for strain sensing tests.

Once the films were annealed, all specimens were prepared for electrical characterization. First, copper tape was affixed onto opposite ends of the film to form a two-point probe measurement setup. Silver paste was also painted over the edge of the copper tape and thin film to ensure complete electrical contact. Then, a digital caliper was used to measure the width and gage length (*i.e.*, the distance between the two electrode) of the film. All films were assumed to be 10 μm thick. Finally, resistance was obtained using an Agilent 34401A digital multimeter (DMM). Calculation of electrical resistivity was based on Eq. 1:

$$\rho = \frac{RA}{L} \tag{1}$$

where ρ is resistivity, R is film resistance, A is the cross-sectional area, and L is the gage length. After measuring the resistivity of all film specimens, the results are summarized in Fig. 3. Fig. 3 plots the average percent decrease in resistivity (and the standard error of the mean) as a function of annealing temperature. The percent decrease in film resistivity corresponding to each annealing temperatures was calculated using Eq. 2:

$$\Delta\rho_{anneal} = -\frac{\rho - \rho_{ave}}{\rho_{ave}} \times 100 \tag{2}$$

where $\Delta\rho_{anneal}$ is the percent change in resistivity of the annealed film and ρ_{ave} is the average resistivity of the non-annealed or control specimens.

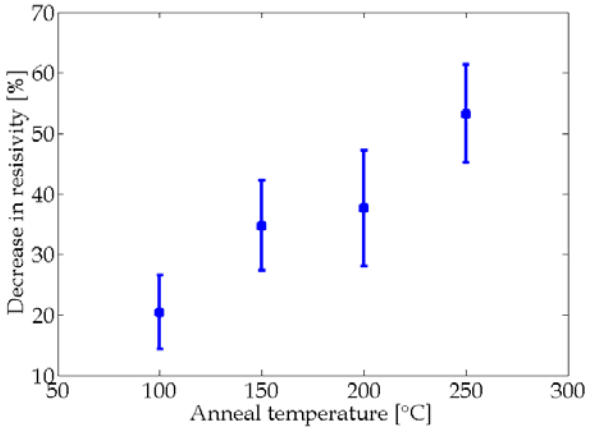

Figure 3: The average decrease in film resistivity as a function of annealing temperature is plotted. Included is also each sample set's standard error of the mean.

One can see from Fig. 3 that, as annealing temperature was increased, the average value of resistivity decreased (*i.e.*, the films became more conductive). This trend is speculated to have resulted from the removal of defects in the films or the melting of PE. It should be mentioned that additional films were annealed at higher temperatures (up to 400 °C), and preliminary results suggested that their electrical and physical properties seemed to degrade. However, due to the few number of specimens tested, the data was not reported. The effects of higher annealing temperatures will be investigated more thoroughly in future studies.

Time-domain Electrical Response. Two-probe resistance measurements of films were measured over several hours in order to observe their transient behavior. For the remaining part of this study, only non-annealed specimens would be used, since more work is required to understand the effects of thermal annealing. As a result of this study, it was found that the spray-fabricated MWNT-based films exhibited fairly stable electrical properties. A representative plot of film resistivity measured over a period of 4,000 s is shown in Fig. 4. It can be seen from Fig. 4 that there was an initial portion where the film resistivity decreases rapidly with time. After approximately 20 min, the film reached its steady-state resistivity and remained within ±1% of this value. Due to the film's sensitivity to temperature, the slight fluctuation in the film's resistivity could be attributed to the slight fluctuation in ambient laboratory temperature.

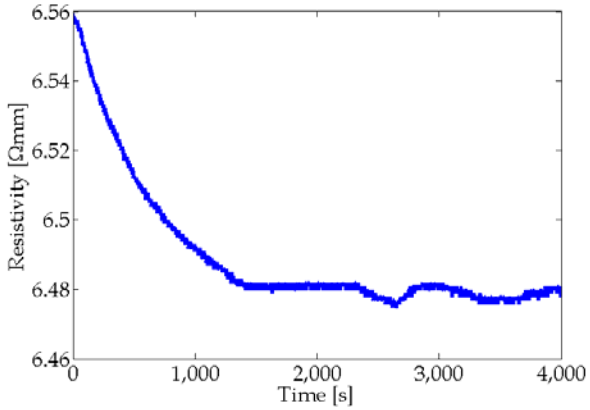

Figure 4: The resistivity of a non-annealed MWNT nanocomposites was measured over time, and its resistivity quickly approached its steady-state value after 20 min.

Electromechanical Response

The electromechanical response of the sprayed MWNT-based films was characterized by measuring their electrical resistance under numerous cycles of tensile strain (up to 10,000 με). First, freestanding nanocomposites were cut into test specimens approximately 1.7×75 mm^2 in size, and conductive copper tape was affixed onto opposite ends of each specimen. Second, the specimen was mounted in a TestResources 150R load frame. It should be noted that the grips (which are electrically insulating) secured the film and electrodes in place to prevent slippage during testing. The load frame was commanded to execute a tensile cyclic load pattern, during which the specimen's electrical resistance was measured using the DMM sampling at 1 Hz. Accuracy of strain measurements were guaranteed by measuring grip displacements using two laser displacement transducers sampling at 20 Hz. Resistance measurements were then converted to resistivity using Eq. 1.

A total of 10 sets of electromechanical tests were conducted using three thin film specimens. A set of representative test results is shown in Fig. 5. In Fig. 5a, good agreement was observed between the resistivity of the thin film and the applied tensile strains. This behavior continued over repeated loading/unloading cycles. Other test results also show similar behavior. Using the raw data plotted to show Fig. 5a, the film's normalized change in resistivity was shown as a function of applied tensile strains in Fig. 5b. Normalized change in resistivity (ρ_n) was calculated using Eq. 3:

$$\rho_n = \frac{\Delta\rho}{\rho_0} \tag{3}$$

where ρ_0 is the film's nominal or initial unstrained resistivity and $\Delta\rho$ is its change in resistivity.

The results from Fig. 5b suggest that there was a linear relationship between the normalized resistivity and the tensile strain; in other words, the film exhibited a linear strain sensing response. A linear least-squares best-fit line was also overlaid in Fig. 5b, and the film's strain sensitivity (S_ε or gage factor) was calculated using the slope of the best-fit line or Eq. 4:

$$S_\varepsilon = \frac{\rho_n}{\varepsilon} \tag{4}$$

where ε is the applied tensile strain.

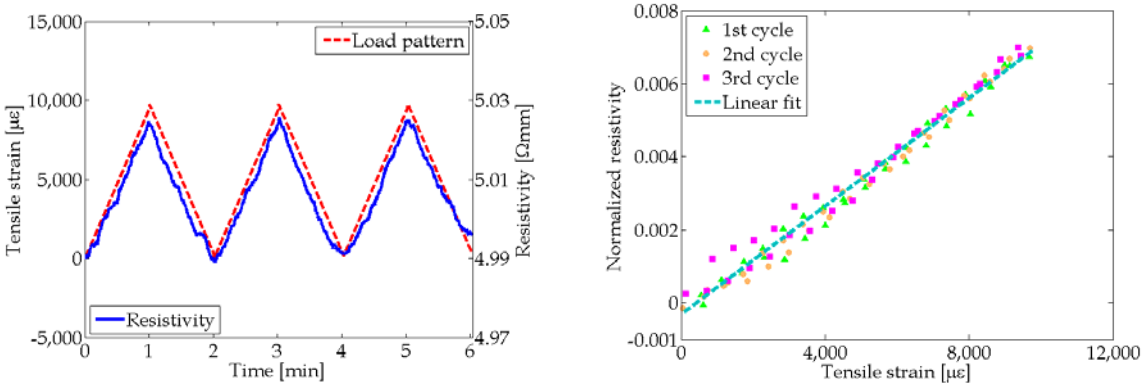

(a) (b)

Figure 5: (a) The strain sensing response of the film is shown by plotting normalized change in resistivity as a function of the applied three-cycle tensile strain load pattern. (b) The same se of data was analyzed, and its normalized resistivity plotted with respect to applied strain shows the film's linear piezoresistivity. The gage factor is approximately 0.77 ± 0.02.

After assessing the strain sensitivities for all the different tests, it was found that the average gage factor (and standard error of the mean) was 0.77 ± 0.02. The gage factor is lower than those reported by Kang *et al.* [16] and Loh *et al*. [10], to name a few. Despite its lower sensitivity, the thin films exhibited high signal-to-noise ratio and high resolution to strain. Similar to Loh *et al.* [17], it is hypothesized that the piezoresistivity of the sprayed MWNT-based thin films resulted from strain-induced changes in the number of electrical conductive pathways. Increasing tensile strains caused a decrease in the number of nanotube-to-nanotube junctions to cause an increase in bulk film resistivity.

Conclusions

This study presented a rapid spray fabrication method for depositing carbon nanotube-based thin film strain sensors. Unlike other nanocomposite techniques, spray fabrication was shown to be scalable, efficient, and low cost. First, films were deposited onto glass substrates, and a subset of films was subjected to thermal annealing (ranging from 100 to 250 °C). Electrical resistivity measurements showed that increasing annealing temperature decreases the film's resistivity; however, this trend was not expected to continue, and preliminary data showed that higher annealing temperatures (400 °C) could degrade film electrical properties. Second, the film's resistivity over time was also recorded. It was found that steady state or nominal resistivity was achieved after approximately 20 min. Finally, freestanding films were prepared and also subjected to strain sensing tests. The results confirmed that sprayed MWNT-based films were piezoresistive, and its average gage factor is 0.77 ± 0.02.

Acknowledgements

This research was supported by the National Science Foundation (grant number CMMI-1200521). The authors would also like to express their gratitude to Dr. Bryan Loyola for his foundational work in spray fabrication of the carbon nanotube-based thin film strain sensors, as well as the support of research collaborator, Prof. Valeria La Saponara.

References

[1] Assembly Committee on Natural Resources, California Senate Bill X1-2, California renewable energy resources act, California Legislature, Sacramento, SB X1-2, 2011.

[2] F. Spinato, P. Tavner, G. Van Bussel, E. Koutoulakos, Reliability of wind turbine subassemblies, IET Renew. Power Gen. 3 4 (2009) 387-401.

[3] T. Verbruggen, Wind turbine operation & maintenance based on condition monitoring: WT-OMEGA, Energy Research Centre of the Netherlands. ECN-C-03-047 ECN (2003).

[4] B. Loyola, V. La Saponara, K.J. Loh, In situ strain monitoring of fiber-reinforced polymers using embedded piezoresistive nanocomposites, J. Mater. Sci. 45 24 (2010) 1-13.

[5] L. Mishnaevsky Jr, P. Brøndsted, R. Nijssen, D. Lekou, T. Philippidis, Materials of large wind turbine blades: Recent results in testing and modeling, Wind Energ. 15 1 (2012) 83-97.

[6] S. Bhalla, C. Kiong Soh, Structural impedance based damage diagnosis by piezo-transducers, Earthq. Eng. Struct. Dyn. 32 12 (2003) 1897-1916.

[7] C.C. Ciang, J.R. Lee, H.J. Bang, Structural health monitoring for a wind turbine system: A review of damage detection methods, Meas. Sci. Technol. 19 12 (2008) 122001 (20 pp).

[8] B.R. Loyola, Y. Zhao, K.J. Loh, V. La Saponara, The electrical response of carbon nanotube-based thin film sensors subjected to mechanical and environmental effects, Smart Mater. Struct. 22 2 (2012) 025010 (11 pp).

[9] K.J. Loh, T.-C. Hou, J.P. Lynch, N.A. Kotov, Carbon nanotube sensing skins for spatial strain and impact damage identification, J. Nondestruct. Eval. 28 1 (2009) 9-25.

[10] K.J. Loh, J. Kim, J.P. Lynch, N. Wong, S. Kam, N.A. Kotov, Multifunctional layer-by-layer carbon nanotube-polyelectrolyte thin films for strain and corrosion sensing, Smart Mater. Struct. 16 2 (2007) 429-438.

[11] B.R. Loyola, Distributed in situ health monitoring of conductive self-sensing fiber-reinforced polymers using electrical impedance tomography, A Ph.D. Thesis, University of California, Davis, Mechanical and Aeronautical Engineering, (2012).

[12] V.C. Moore, M.S. Strano, E.H. Haroz, R.H. Hauge, R.E. Smalley, Individually suspended single-walled carbon nanotubes in various surfactants, Nano Lett. 3 (2003) 1379-1382.

[13] S.D. Bergin, V. Nicolosi, P.V. Streich, S. Giordani, Z. Sun, A.H. Windle, P. Ryan, N.P.P. Niraj, Z.-T.T. Wang, L. Carpenter, W.J. Blau, J.J. Boland, J.P. Hamilton, J.N. Coleman, Towards solutions of single-walled carbon nanotubes in common solvents, Adv. Mater. 20 10 (2008) 1876-1881.

[14] R.H. Hansen, H. Schonhorn, A new technique for preparing low surface energy polymers for adhesive bonding, J. Polym. Sci. Part B Polym. Lett. 4 3 (1966) 203-209.

[15] M. Kosaka, T.W. Ebbesen, H. Hiura, K. Tanigaki, Annealing effect on carbon nanotubes. An ESR study, Chem. Phys. Lett. 233 1-2 (1995) 47-51.

[16] I. Kang, M.J. Schulz, Y.S. Choi, S.H. Hwang, Carbon nanotube composites multi-sensing characteristics based on electrical impedance properties, J. Nanosci. Nanotechnol. 9 12 (2009) 7364-7367.

[17] K.J. Loh, J.P. Lynch, B.S. Shim, N.A. Kotov, Tailoring piezoresistive sensitivity of multilayer carbon nanotube composite strain sensors, J. of Intell. Mater. Syst. and Struct. 19 7 (2008) 747-764.